

A Photometric Method to Search for Be Stars in Open Clusters

M. Virginia McSwain^{1,2,3} and Douglas R. Gies

Department of Physics and Astronomy, Georgia State University, P.O. Box 4106, Atlanta, GA 30302-4106
 mcswain@astro.yale.edu, gies@chara.gsu.edu

ABSTRACT

We describe a technique to identify Be stars in open clusters using Strömgren b , y , and narrow-band $H\alpha$ photometry. We first identify the B-type stars of the cluster using a theoretical isochrone fit to the $(b-y, y)$ color-magnitude diagram. The strongest Be stars are easily identified in a $(b-y, y - H\alpha)$ color-color diagram, but those with weaker $H\alpha$ emission (classified as possible Be star detections) may be confused with evolved or foreground stars. Here we present such photometry plus $H\alpha$ spectroscopy of members of the cluster NGC 3766 to demonstrate the accuracy of our technique. Statistical results on the relative numbers of Be and B-type stars in additional clusters will be presented in a future paper.

Subject headings: stars: emission-line, Be — open clusters and associations: individual(NGC 3766) — techniques: photometric

1. Introduction

Be stars are broadly defined as non-supergiant (luminosity class III–V) B-type stars that show or have shown Balmer emission (Porter & Rivinius 2003), although a few supergiant Be stars are also known (Negueruela 2004). Their emission is due to a circumstellar disk that is often highly variable on both short and long time scales. The emission lines change intensity, and the relative intensity of their double-peaked profiles changes, over short time scales of days and even hours. In addition, the disks themselves have been observed to disappear and reappear over years or decades (Slettebak 1988). Be stars are well known to be a class of rapidly rotating stars (Slettebak 1949, 1966; Slettebak, Collins, & Truax 1992), and there are three possible reasons for their rapid rotation. They may have been born as rapid rotators (Zorec & Briot 1997), spun up by binary mass transfer (Pols et al. 1991), or spun up during the main-

sequence (MS) evolution of B stars (Meynet & Maeder 2000; Fabregat & Torrejón 2000).

Many observational surveys have searched for Be stars in open clusters using multi-band photometry. Shobbrook (1985, 1987) used plots of c_1 vs. β , c_1 vs. V magnitude, and β vs. V to identify Be stars in NGC 3766. Many recent surveys have relied on color-color diagrams, rather than Shobbrook’s color-magnitude diagrams, to detect Be stars more efficiently. Grebel, Richtler, & de Boer (1992) used a technique somewhat similar to ours (§3) to identify Be stars in NGC 330. They used Strömgren b, y , and a narrow-band $H\alpha$ filter for their observations, and they plotted a color-color diagram for the cluster using $b-y$ vs $H\alpha-y$. They were able to verify almost all of their detections with low resolution spectra, demonstrating the accuracy of this technique. Several other surveys (Grebel 1997; Dieball & Grebel 1998; Keller, Wood, & Bessell 1999; Keller, Bessell, & Da Costa 2000; Grebel & Chu 2000; Pigulski, Kopacki, & Kołaczowski 2001) have used variations of the color-color diagram technique to identify Be stars in open clusters. Grebel (1997) emphasizes that the number of Be stars detected in this type of surveys actually represents a lower limit on the

¹Current address: Department of Astronomy, Yale University, P.O. Box 208101, New Haven, CT 06520-8101

²Visiting Astronomer, Cerro Tololo Inter-American Observatory. CTIO is operated by AURA, Inc. under contract to the National Science Foundation.

³NSF Astronomy and Astrophysics Postdoctoral Fellow

true number of Be stars for several reasons. Most importantly, since the Be state is not permanent, only those stars with current disk outbursts will be detectable as Be stars. In addition, the number of late type Be stars is likely to be incomplete since they are fainter, and they also tend to have weaker $H\alpha$ emission than early Be stars.

In this paper, we present an improved photometric technique based on $(b - y, y)$ color-magnitude and $(b - y, y - H\alpha)$ color-color diagrams to detect Be stars in open clusters. While our method is very similar to that of Grebel et al. (1992), we have enhanced it by using cluster isochrone fitting to identify the B-type stars in each cluster. We have also used a fit of the color-color curve to identify $H\alpha$ emitters among the B star population. To demonstrate the accuracy of our technique, we present spectra of 20 stars in the cluster NGC 3766 and correlate their $H\alpha$ equivalent widths with their $y - H\alpha$ colors. Our photometry of additional clusters will be presented in a future paper, and at that time we will use our statistics to discuss the implications on the possible Be star formation scenarios.

2. Observations

We made photometric observations of the cluster NGC 3766 on 2002 April 1 using the CTIO 0.9 m telescope with the SITe 2048 CCD. The images were binned using a CCD summing factor of 2×2 pixels due to the slow readout time of the chip. Without binning, the chip has a plate scale of $0.401''/\text{pixel}$, but with binning the plate scale increased by a factor of 2.

We observed the cluster using Strömgren b and y filters as well as a narrow band $H\alpha$ filter, and we obtained two observations of 5 s duration in each filter. We also observed five standard stars (HD 79039, HD 80484, HD 104664, HD 105498, and HD 128726) from the list of Cousins (1987). Each standard star was observed in each band at a minimum of three different airmasses. All of the images were processed in IRAF¹ using nightly bias and dome flat frames, and we used the technique described by Massey & Davis (1992) to compute

the instrumental magnitudes of each object. We determined the magnitudes of the standard stars using a large aperture of $8''$, and we used a smaller aperture for the more crowded cluster stars and later performed an aperture correction to transform the target measurements to the aperture system of the standards.

We calibrated our Strömgren b and y photometry of NGC 3766 using the photometric transformation equations from Henden & Kaitchuck (1982), but the $H\alpha$ magnitudes were somewhat harder to correct since the filter system is not universally standard. We corrected the $H\alpha$ instrumental magnitudes for atmospheric extinction by plotting each standard star's instrumental magnitude vs. airmass, and the slope provides a good measure of the principal extinction coefficient. Since the color coefficient is difficult to determine without knowing the absolute $H\alpha$ magnitudes, and since color is relatively unimportant for the response of such a narrow-band filter, we assumed it to be negligible within errors. We also assumed that the second-order term is zero. We determined the constant offset between the instrumental $H\alpha$ magnitudes and the true magnitudes by fitting a theoretical color-color curve to the MS B stars in the observed color-color diagram (described in §3). Because the theoretical curve assumes that Vega, an A0 V star, is assigned a magnitude of zero, the final $H\alpha$ magnitudes are calibrated using this convention. The errors in the magnitudes are from the combined estimated instrumental errors, the standard deviation of the aperture correction, and the errors in the transformation coefficients. They are usually < 0.04 mag in b and y , and < 0.07 mag in $H\alpha$. Our photometry of NGC 3766 is listed in Table 1, which is available online (see Note to Table 1).

From our images, we also performed astrometry of the cluster to determine accurate positions of each star. Ten medium-bright stars from each cluster were selected to be astrometry reference stars, and we matched their average (x, y) positions with their right ascension, α , and declination, δ , from the 2MASS All-Sky Catalog of Point Sources (Cutri et al. 2003). We used the IDL routine *astromit.pro*, written by R. Cornett & W. Landsman, to compute the astrometric solution from the reference stars. With this known solution, the program *uit_xy2ad.pro*, written by R.

¹IRAF is distributed by the National Optical Astronomy Observatory, which is operated by the Association of Universities for Research in Astronomy, Inc., under cooperative agreement with the National Science Foundation.

Cornett, B. Boothman and J. D. Offenberg, used the list of (x, y) positions of all stars in NGC 3766 and output their α and δ . Using this technique, we obtained typical errors of $0''.10$ in both $\alpha \cos \delta$ and δ .

In addition, we obtained spectra of 21 members of NGC 3766 with the CTIO 1.5 m telescope in 2003 March. These first-order spectra were made with the Cassegrain spectrograph, the #47 grating (831 grooves mm^{-1} , blazed at 8000 Å), a GG495 order sorting filter, and a Loral 1200×800 CCD. This arrangement recorded the spectrum over the range 5490 – 6790 Å with a resolving power of $\lambda/\Delta\lambda = 1700$. Exposure times varied between 300 – 1800 s, and resulted in a $S/N = 300$ pixels $^{-1}$ near $H\alpha$. We did not remove the weak, narrow telluric lines from these spectra so that our measurements of the line flux more closely correspond to the photometric measurements. These spectra were reduced to a rectified intensity versus heliocentric wavelength format using standard procedures in IRAF.

3. Detection Technique

Figure 1 shows a color-magnitude diagram of NGC 3766 with the theoretical isochrone, assuming solar metallicity, from Lejeune & Schaerer (2001). For this cluster, we used the values of the reddening, $E(b - y) = 0.15$, and unreddened distance modulus, $5 \log d - 5 = 11.4$, provided by Shobbrook (1985) and $\log \text{age (years)} = 7.16$ from the WEBDA database for Galactic open clusters². However, Lejeune & Schaerer do not include an isochrone for this cluster age in their database, so we used the closest match ($\log \text{age} = 7.15$) in Figure 1. Because their models do not provide Strömgren magnitudes, we transformed the Johnson V magnitude to Strömgren y using the transformation

$$y = V - 0.038(B - V) \quad (1)$$

(Cousins & Caldwell 1985). To transform $B - V$ to $b - y$, we used

$$B - V = 1.584(b - y) + 0.681m_1 - 0.116 \quad (2)$$

from Turner (1990). Not having obtained the v magnitudes for the cluster, we used the ZAMS re-

lation from Perry et al. (1987) to find appropriate values of m_1 for different values of $b - y$, and we interpolated between them for all other values of $b - y$.

Each point along the theoretical isochrone corresponds to an effective temperature, and we defined all objects with temperatures between 10000 – 30000 K as B stars. Some B-type giants and supergiants may be included in this range as a result. The horizontal dashed line in Figure 1 represents the maximum magnitude for B-type stars in the cluster, y_{Bmax} , while the minimum B star magnitude, y_{Bmin} , is out of the plot range. The massive O- and B-type stars all lie to the left of the vertical dashed line that represents $E(b - y)$. It is important to note that the gap between the faintest stars and the horizontal line y_{Bmax} may indicate a systematic bias in this search for Be stars; in NGC 3766, our photometry does not detect the faintest late-type B or Be stars.

Before inspecting the observed color-color curve of NGC 3766, we created a theoretical color-color curve using colors derived from Kurucz (1979) model spectra. These model flux distributions include a realistic treatment of the $H\alpha$ line profile, and they have a fine enough resolution to permit a reasonable estimate of the flux that passes through the narrow-band $H\alpha$ filter (about 5 model wavelength points span the full range of the filter). We used the IRAF routine *calcphot* in the *HST stsdas/synphot* package to calculate the $y - H\alpha$ and $b - y$ indices for the Kurucz model fluxes assuming solar metallicity, $\log g = 4.0$ and 4.5 , and a temperature range of 7000 – 30000 K. We omitted higher temperature, O-type stars because non-LTE effects become important in these stars, and Balmer line absorption is stronger than predicted by the Kurucz LTE models. We had to adjust the Strömgren b and y magnitudes from *calcphot* for the true magnitudes of the A0 V star Vega since they differ slightly from zero in the Strömgren system (Gray 1998; Hauck & Mermilliod 1998). We then interpolated between the two gravity models $\log g = 4.0$ and 4.5 for the gravity associated with MS stars in the Lejeune & Schaerer (2001) models. The solid line in Figure 2 shows the resulting theoretical color-color curve from the Kurucz model spectra. Along this curve, the $y - H\alpha$ index rises with $b - y$ color in redder (cooler) stars, and the curve has a local minimum near $b - y = 0.0$ that

²The WEBDA database is maintained by J.-C. Mermilliod and is available online at obswwww.unige.ch/webda/navigation.html.

corresponds to the maximum H Balmer absorption line strength found in early A-type stars. The dashed line in Figure 2 represents the same Kurucz model colors at a reddening of $E(B - V) = 0.5$ using the reddening law from Fitzpatrick (1999) for an assumed value of $R \equiv A(V)/E(B - V) = 3.1$. Note that for this value of R , $E(B - V)$ can be converted to the Strömngren system using the expression

$$E(b - y) = 0.745 \times E(B - V) \quad (3)$$

from Fitzpatrick (1999).

Figure 2 also includes the color indices derived from dereddened spectra of 161 stars from the atlas of Jacoby, Hunter, & Christian (1984). There appears to be good agreement between the reference color-color relation from the Kurucz fluxes and the observed colors of MS stars in the B- and A-type spectral range ($b - y = -0.13$ to 0.25). The mean difference is $(y - H\alpha)_{\text{obs}} - (y - H\alpha)_{\text{mod}} = 0.01 \pm 0.05$, where the error indicates the standard deviation. The most discrepant point is 0.10 mag away from the predicted trend. This indicates that the reference curve can be applied to our photometry with relatively small systematic errors. However, it does point out the need to be cautious in identifying Be stars. Hot, post-MS stars have slightly larger $y - H\alpha$ indices than MS stars since they have narrower $H\alpha$ absorption profiles due to less pressure broadening in their atmospheres. In addition, unreddened MS stars may appear slightly above the reddened theoretical curve and could be confused with weak Be stars. A parabolic fit of the colors of the entire Jacoby et al. sample is shown as a dotted curve, and unreddened foreground stars will probably be found close to this line in the observed color-color diagrams.

It was difficult to match the theoretical color-color curve to the observed data, however, since the model assumes $y - H\alpha = 0$ for A0 V stars (specifically, Vega), but the $H\alpha$ photometry was not initially calibrated to such a standard system. Therefore, we used the B star data to find the average difference between our data and the model, and we offset the $H\alpha$ magnitudes by adding this difference. Because the fit was sometimes skewed by Be stars with significantly larger $y - H\alpha$ values, we removed any stars more than 2σ above the fit and improved the offset. Here, σ is the standard

deviation of the $y - H\alpha$ residuals from the Kurucz relation for the stars in NGC 3766.

The color-color diagram of NGC 3766 is plotted in Figure 3, which also includes the theoretical color-color curve (solid line) transformed according to the adopted reddening $E(b - y)$ for the cluster using the reddening law from Fitzpatrick (1999). The long dashed line in the diagram is the parabolic fit for unreddened MS and evolved stars from the Jacoby et al. sample. Finally, the vertical dotted line in Figure 3 indicates $E(b - y)$.

With theoretical models correlated to both the color-magnitude and color-color diagrams, we used the agreement to identify both B stars and Be stars among the cluster members. The B stars lie in the region $y_{B\text{min}} < y < y_{B\text{max}}$ and $b - y < E(b - y)$. A subset of these B stars may be active Be stars, which are distinguished by their line emission, often in $H\alpha$, so they will usually appear brighter in this band than normal B stars. Those B stars with $y - H\alpha$ more than 2σ above the theoretical color-color curve (and above the unreddened MS fit, to eliminate unreddened foreground stars and post-MS stars) are tentatively classified as Be stars. Each Be star candidate is represented with a large diamond in Figures 1 and 3, whereas all other stars are shown as small diamonds. Definite Be star detections are those candidates which have a significantly larger ($> 5\sigma$) $y - H\alpha$ color than the cluster's B-type population. The possible detections are those whose colors lie just slightly above the unreddened MS fit. These possibly include some contaminating foreground stars and supergiants, but we show in §4 that this population does include some weakly emitting Be stars.

4. Spectroscopic Test of the Method

To test the accuracy of this photometric method of identifying Be stars in NGC 3766, we performed a spectroscopic investigation of this cluster. From a literature search, we found 22 previously identified Be stars in NGC 3766. Mermilliod (1982) lists 13 Be stars identified by $H\alpha$ line emission in their spectra, and Shobbrook (1985, 1987) classified 10 of Mermilliod's stars plus 9 additional stars as Be stars based on his own Strömngren $uvby$ and $H\beta$ photometry.

Our own color-color diagram of NGC 3766,

shown in Figure 3, revealed only 5 Be stars with definite H α emission (WEBDA #15, 264, 240, 88, and 53). In addition to these, one of the previously identified Be stars (#232) was saturated in our images, and one was not in the field-of-view (#301). To resolve the discrepancy between the published literature and our results, we obtained spectra of these previously identified Be stars, excluding only the star outside the field-of-view in our CCD images.

From the spectra of NGC 3766, we found that only 9 of the 21 stars exhibited H α emission in our spectra. One of these emission stars (#232) was indeed the known Be star that is saturated in the photometry. We show the relative H α profiles of the other 8 emission stars in NGC 3766, offset vertically for clarity, in Figure 4. Five of these 8 stars, those with the strongest H α emission, are easily identified as Be stars in the color-color diagram in Figure 3. Therefore, our technique for identifying definite Be star candidates with a $b - y$ vs $y - \text{H}\alpha$ diagram accurately accounts for about 63% of the Be stars in this cluster.

The three Be stars that did not stand out in the color-color diagram each had somewhat different H α line profiles from the other Be stars. One star (#1) had a “shell” spectrum, i.e., weak emission in the wings of the line accompanied by stronger central absorption. This line profile is characteristic of Be stars observed nearly edge-on, so that the thick hydrogen disk absorbs an even larger fraction of the star’s flux at H α . The other two Be stars (#27 and #151 southern component) had only weak H α emission, probably from smaller disks, making it more difficult to distinguish them from non-emission stars.

After reviewing the results from the spectra, we looked more carefully at Figure 3 and noticed a group of stars occupying a region just slightly above the bulk of the OB stars, but beneath the unreddened line that we use as the cutoff for Be star detections. These may be weak H α emitters, or they may be foreground stars. Within the errors of the photometry, this group is nearly indistinguishable from the non-emitters. The shell star #1 was in this group, so it was not detected as a Be star candidate. However, the weak emitter #27 was found just above the unreddened line, so it was identified as a possible Be star by our technique. The final weak emitter, #151, was

grouped with the non-emitting OB stars in the color-color diagram. On the other hand, two stars that did not show H α emission in the spectra, #26 and #204, appeared as possible Be star detections above the unreddened line. Given that the weakly-emitting Be stars and the non-emitting B star regions overlap within the errors of the photometry, it is easy to attribute the confusion to the photometry errors. However, it is worth noting that #26 and #204 have been classified as Be stars in the past, and there was a one year gap between obtaining photometry and spectroscopy of this cluster. Therefore it is also possible to attribute the discrepancy between the photometry and spectroscopy to intermittent weak emission from these stars. Therefore we count each of the stars in the weakly-emitting region of the color-color diagram as possible Be star detections, but we do not include #1 or #151 as a detection based on the criteria discussed above.

Twelve of the previously identified Be stars in NGC 3766 did not have active H α emission at the time of our spectroscopic observations. We show their H α absorption profiles in Figure 5 on a slightly different scale than Figure 4. Several of these stars (especially #291, 204, 195, 146, 36, and 4) have absorption line profiles that may have a small emission component in the absorption line cores due to weak nebular H α emission. Alternatively, the emission-like profile could be an indication of line blending in double-line spectroscopic binaries. This superposition of two absorption line profiles can mimic Be star emission profiles; Coté & van Kerkwijk (1993) found that several stars in their Be star sample had been misclassified as emission stars due to their binary nature. More spectra of these stars are needed to confirm if they are indeed spectroscopic binaries that have been misclassified as Be stars in the past.

To demonstrate the overall accuracy of this technique to identify Be stars, we show in Figure 6 a plot of the equivalent width, W_λ , of H α versus the $y - \text{H}\alpha$ color of the 20 stars with both photometry and spectroscopy. W_λ was measured by performing a numerical integration from 6529 – 6597 Å, the range covered by the narrow band H α filter (FWHM = 68 Å, centered at 6567 Å). The measurement errors are dominated by the placement of the continuum and amount to $\delta W_\lambda = \pm 0.22$ Å or better. Absorption features have positive equiv-

alent width while emission features have negative equivalent width, but the equivalent width may be positive for weak emission line stars in which the emission only partially fills the photospheric absorption line of $H\alpha$. We fit the observed W_λ and $y - H\alpha$ color to the logarithmic relationship

$$y - H\alpha = C + 2.5 \log \left(\frac{\text{FWHM}_{H\alpha} - W_\lambda}{\text{FWHM}_{H\alpha}} \right) \quad (4)$$

with the fitting factor $C = 0.264$, and this curve is shown as a solid line in Figure 6. There is significant scatter in the observed relationship compared to the theoretical curve, and the boundary between Be and non-Be stars is unclear, probably due to the variability of $H\alpha$ emission over the year between our observations. However, Be stars appear to have $y - H\alpha \gtrsim 0.2$ in our calibrated system.

5. Conclusions

Our photometric technique for identifying Be stars is very efficient for finding those stars with strong $H\alpha$ emission, as we have shown for NGC 3766. While we correctly identify 63% of the previously known, currently active Be stars in NGC 3766, we do not confirm the active Be status of 7 stars claimed as Be stars in the past. As our results show, Be stars with weaker emission are more difficult to identify conclusively with the color-color diagram method. Even if the errors in the photometry were negligible, these stars may be confused with unreddened foreground stars or supergiants in a color-color diagram. In some cases it may be possible to eliminate such foreground stars from the sample based on their positions relative to the MS in a color-magnitude diagram; alternatively, proper motions or radial velocities may be used to separate non-members from the cluster sample. We do not think that B-type supergiants are a significant source of contamination since supergiants within the cluster will be rejected by the y_{Bmin} constraint in the color-magnitude diagram, and the chances of having a background B supergiant in the sample are very small unless two distant clusters fall along the same line of sight (this is the case with some of the clusters in our forthcoming paper). However, B-type supergiants can be removed from the sample by including IR photometry in the observational program since Be star disks will create an IR excess that is correlated

to their luminosity in $H\alpha$ (Stee & Bittar 2001). If such measurements are not available, $H\alpha$ spectroscopy may be required to conclusively identify weak $H\alpha$ emitters.

As Figure 1 shows, our photometry of NGC 3766 does not cover the entire range of B star magnitudes. Unless the observational program is designed to reach A-type stars, the total number of B, and perhaps Be, stars will be underestimated in any search for Be stars. This is especially a concern when measuring the fraction of Be stars relative to normal B-type stars because the number of B-type stars increases dramatically with later spectral types. Keller et al. (2001) illustrate this problem with their deep photometric survey of the clusters h and χ Persei. They find that more than 30% of the brightest B stars are Be stars, but the Be star fraction decreases to 2% or less for B5–B9 spectral types. Because many other studies of Be stars (e.g. Mermilliod 1982; Shobbrook 1985; Grebel 1997; Fabregat & Torrejón 2000) rely upon magnitude limited samples that do not accurately reflect the true Be fractions, this source of incompleteness is worth discussion. However, in this situation a more accurate Be/B star fraction can be determined by assuming a typical IMF distribution for the cluster and extrapolating to estimate the number of late stars omitted. As Keller et al. (2001) show, the contribution of late-type Be stars is small and may be neglected in such an extrapolation.

Both Abt (1987) and Grebel (1997) have discussed another problem with short-term photometric studies of Be stars, namely that they only detect those Be stars with active emission at the time of the observations, and thus only a lower limit of the true Be population is found. This effect can be significant in observational surveys; Coté & van Kerkwijk (1993) found that 14% of the known Be stars in their sample of B stars from the Bright Star Catalogue did not show active emission. From our own spectra of NGC 3766, we found that only 9 of 21 Be stars discussed in the literature had active disks in 2003 March, although we believe that at least some of these Be stars have been misidentified in the past. From these two studies, the true fractions of Be stars in a sample could be anywhere between 1.2 – 2.3 times the number detected. Only a long term, multi-year investigation will approach the complete population

of Be stars in a given sample.

While our $(b-y, y-H\alpha)$ color-color technique is limited in its ability to detect weakly emitting Be stars, this is still an efficient method for identifying Be stars in open clusters. Applied consistently to a large sample of open clusters, the variability of the Be phenomenon can be neglected and this technique can provide important statistical results about these stars, especially regarding their evolutionary status and the cause of their rapid rotation. In an upcoming paper, we will apply our photometric method to more than 50 additional clusters and discuss the results.

We are grateful to the SMARTS Consortium for our observing time with the CTIO 1.5m telescope. MVM thanks NOAO for travel support to observe with the CTIO 0.9m telescope. MVM is supported by an NSF Astronomy and Astrophysics Postdoctoral Fellowship under award AST-0401460. Financial support also was provided by the NSF through grant AST-0205297 (DRG). Institutional support has been provided from the GSU College of Arts and Sciences and from the Research Program Enhancement fund of the Board of Regents of the University System of Georgia, administered through the GSU Office of the Vice President for Research.

Facilities: CTIO.

REFERENCES

- Abt, H. A. 1987, in *Physics of Be Stars*, ed. A. Slettebak & T. P. Snow (Cambridge: Cambridge Univ. Press), 470
- Coté, J., & van Kerkwijk, M. H. 1993, *A&A*, 274, 870
- Cousins, A. W. J. 1987, *South African Astron. Obs. Circ.*, 11, 93
- Cousins, A. W. J., & Caldwell, J. A. R. 1985, *Obs.*, 105, 134
- Cutri, R. M., et al. 2003, *The 2MASS All-Sky Catalog of Point Sources* (Pasadena: Univ. Mass. & IPAC)
- Dieball, A., & Grebel, E. K. 1998, *A&A*, 339, 773
- Fabregat, J., & Torrejón, J. M. 2000, *A&A*, 357, 451
- Fitzpatrick, E. L. 1999, *PASP*, 111, 63
- Gray, R. O. 1998, *AJ*, 116, 482
- Grebel, E. K. 1997, *A&A*, 317, 448
- Grebel, E. K., & Chu, Y.-H. 2000, *AJ*, 119, 787
- Grebel, E. K., Richtler, T., & de Boer, K. S. 1992, *A&A*, 254, L5
- Hauck, B., & Mermilliod, M. 1998, *A&AS*, 129, 431
- Henden, A. A., & Kaitchuck, R. H. 1982, *Astronomical Photometry* (New York: Van Nostrand Reinhold Company)
- Jacoby, G. H., Hunter, D. A., & Christian, C. A. 1984, *ApJS*, 56, 257
- Keller, S. C., Bessell, M. S., & Da Costa, G. S. 2000, *AJ*, 119, 1748
- Keller, S. C., Grebel, E. K., Miller, G. J., & Yoss, K. M. 2001, *AJ*, 122, 248
- Keller, S. C., Wood, P. R., & Bessell, M. S. 1999, *A&AS*, 134, 489
- Kurucz, R. L. 1979, *ApJS*, 40, 1
- Lejeune, T., & Schaerer, D. 2001, *A&A*, 366, 538
- Massey, P., & Davis, L. E. 1992, *A User's Guide to Stellar CCD Photometry with IRAF* (Tucson: NOAO), online at <http://iraf.noao.edu/docs/photom.html>
- Mermilliod, J.-C. 1982, *A&A*, 109, 48
- Meynet, G., & Maeder, A. 2000, *A&A*, 361, 101
- Negueruela, I. 2004, *Astron. Nachr.*, 325, 380
- Perry, C. L., Olsen, E. H., & Crawford, D. L. 1987, *PASP*, 99, 1184
- Pigulski, A., Kopacki, G., & Kołaczkowski, Z. 2001, *A&A*, 376, 144
- Pols, O. R., Coté, J., Waters, L. B. F. M., & Heise, J. 1991, *A&A*, 241, 419
- Porter, J. M., & Rivinius, T. 2003, *PASP*, 115, 1153
- Shobbrook, R. R. 1985, *MNRAS*, 212, 591

- Shobbrook, R. R. 1987, MNRAS, 225, 999
- Slettebak, A. 1949, ApJ, 110, 498
- Slettebak, A. 1966, ApJ, 145, 126
- Slettebak, A. 1985, ApJS, 59, 769
- Slettebak, A. 1988, PASP, 100, 770
- Slettebak, A., Collins, G. W., II, & Truax, R.
1992, ApJS, 81, 335
- Stee, Ph., & Bittar, J. 2001, A&A, 367, 532
- Townsend, R. H. D., Owocki, S. P., & Howarth, I.
D. 2004, MNRAS, 350, 189
- Turner, D. G. 1990, PASP, 102, 1331
- Zorec, J., & Briot, D. 1997, A&A, 318, 443

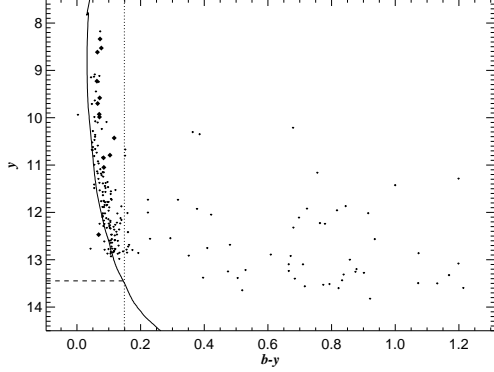


Fig. 1.— Color-magnitude diagram of the cluster NGC 3766. The isochrone fit (*solid line*), $E(b-y)$ (*dotted line*), and y_{Bmax} (*dashed line*) are discussed in the text. Be stars (*large*) are distinguished from all other stars (*small*) in the diagram.

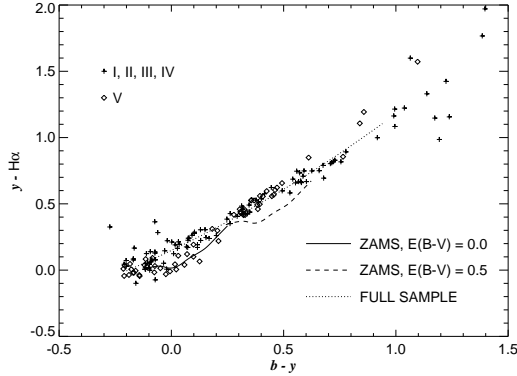


Fig. 2.— The theoretical unreddened color-color curve (*solid line*) and reddened curve (*dashed line*) derived from Kurucz (1979) model spectra are plotted. In addition, the colors of 161 MS (*diamonds*) and more luminous stars (*plus signs*) from the atlas of Jacoby et al. (1984) are shown. The parabolic fit of these stars' colors is also shown (*dotted line*).

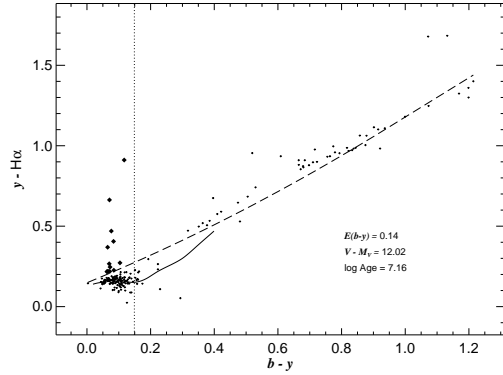


Fig. 3.— Color-color diagram of the cluster NGC 3766. The color-color fit from the Kurucz model fluxes (*solid line*), the parabolic fit for unreddened MS and evolved stars from Jacoby et al. (1984) (*dashed line*), and $E(b-y)$ (*dotted line*) are also indicated. The Be stars are distinguished in the same format as Figure 1.

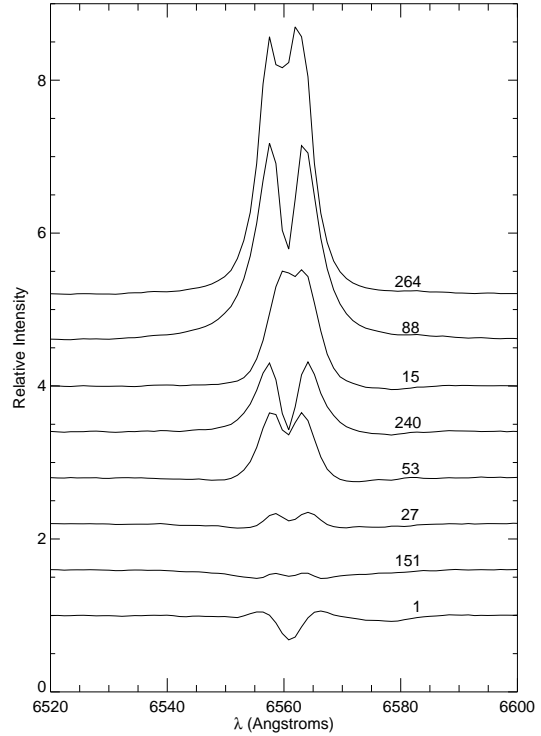


Fig. 4.— The relative $H\alpha$ profiles are shown for 8 Be stars in NGC 3766, labeled by their WEBDA number. The relative intensities are offset vertically for clarity.

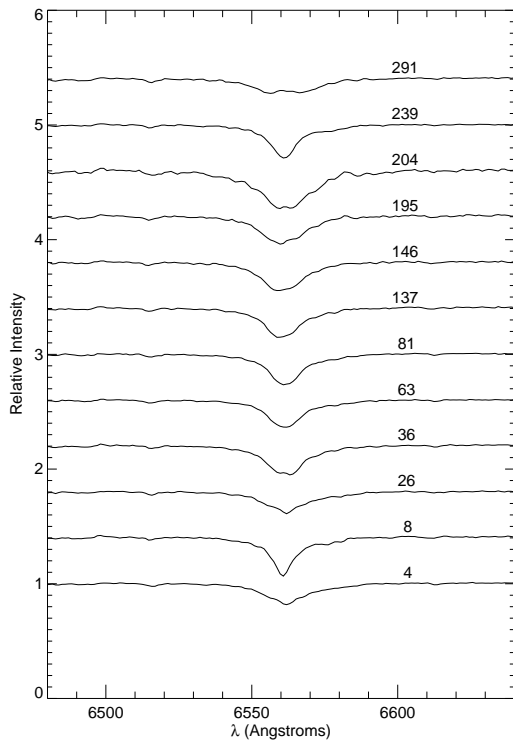


Fig. 5.— The relative $H\alpha$ profiles are shown for 12 inactive Be stars in NGC 3766 in the same format as Figure 4.

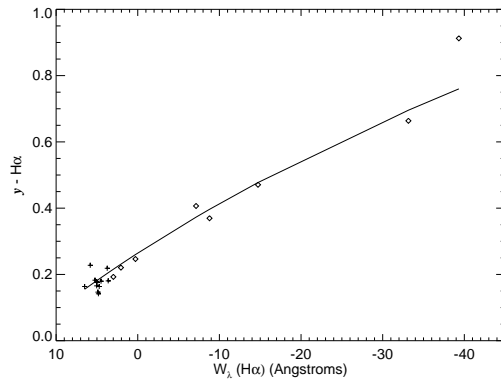


Fig. 6.— The $H\alpha$ equivalent widths from our spectra are shown plotted against the observed $y - H\alpha$ color from our photometry for 20 stars in NGC 3766. Stars with $H\alpha$ emission in their spectra indicating that they are Be stars (*diamonds*) generally have a higher $y - H\alpha$ color index and more negative W_λ than non-Be stars (*crosses*). The theoretical logarithmic relationship between W_λ and $y - H\alpha$ is also shown as a solid line.

TABLE 1
PHOTOMETRY OF NGC 3766

Star	RA (2000)	Dec (2000)	y	δy	$b - y$	$\delta(b - y)$	$y - H\alpha$	$\delta(y - H\alpha)$	Code	WEBDA	Identifier
1	11 35 59.26	-61 29 14.3	12.787	0.034	0.087	0.043	0.119	0.075	O
2	11 35 48.57	-61 29 19.2	9.708	0.011	0.047	0.016	0.174	0.031	B
3	11 36 56.50	-61 29 18.9	12.912	0.035	0.351	0.047	0.498	0.069	O
4	11 36 18.84	-61 29 32.3	12.856	0.035	0.193	0.045	0.295	0.073	O	156	...
5	11 35 14.04	-61 29 46.4	12.002	0.024	0.222	0.033	0.233	0.054	O
6	11 36 43.71	-61 30 04.1	11.866	0.025	0.844	0.039	0.987	0.044	O
7	11 35 28.04	-61 30 24.7	12.108	0.027	0.698	0.040	0.880	0.049	O
8	11 35 59.95	-61 30 26.6	11.484	0.020	0.090	0.026	0.146	0.047	B
9	11 36 23.12	-61 30 28.9	13.078	0.041	1.199	0.066	1.360	0.062	O
10	11 35 41.55	-61 30 39.6	13.384	0.059	0.505	0.081	0.684	0.106	O	303	...
11	11 36 15.81	-61 30 50.3	11.763	0.022	0.085	0.029	0.166	0.049	B
12	11 35 53.33	-61 30 59.6	13.095	0.039	0.665	0.055	0.911	0.066	O
13	11 36 08.00	-61 31 00.6	12.751	0.033	0.409	0.045	0.576	0.064	O
14	11 36 55.10	-61 31 06.3	12.319	0.029	0.680	0.042	0.866	0.051	O
15	11 36 17.65	-61 31 27.1	11.918	0.026	0.723	0.039	0.900	0.047	O	160	...
16	11 36 41.89	-61 31 37.3	9.145	0.011	0.044	0.016	0.154	0.030	B	169	HD 100969
17	11 35 26.03	-61 31 39.0	13.594	0.049	1.214	0.077	1.401	0.074	O	294	...
18	11 36 54.78	-61 31 49.5	12.564	0.033	0.935	0.051	1.109	0.054	O	173	...
19	11 36 06.15	-61 31 52.9	10.210	0.017	0.679	0.027	0.873	0.033	O	147	...
20	11 36 09.17	-61 31 55.7	11.386	0.019	0.081	0.025	0.169	0.045	B	148	...
21	11 36 43.90	-61 31 59.0	13.197	0.041	0.878	0.062	1.063	0.069	O	170	...
22	11 35 31.46	-61 32 07.1	12.415	0.029	0.160	0.038	0.167	0.064	O
23	11 36 56.37	-61 32 08.5	12.768	0.033	0.119	0.043	0.213	0.069	B
24	11 36 07.96	-61 32 10.5	13.311	0.041	0.837	0.062	0.983	0.071	O	149	...
25	11 35 22.07	-61 32 10.9	10.736	0.016	0.062	0.021	0.179	0.038	B	291	HD 306793
26	11 36 00.76	-61 32 22.7	11.752	0.022	0.084	0.028	0.173	0.050	B	145	...
27	11 35 55.73	-61 32 32.0	11.152	0.018	0.084	0.024	0.183	0.041	B	146	...
28	11 35 48.24	-61 32 33.9	12.288	0.026	0.102	0.034	0.130	0.060	B	134	...
29	11 36 12.51	-61 32 40.2	10.281	0.014	0.050	0.020	0.147	0.035	B
30	11 35 28.63	-61 32 42.3	12.840	0.034	0.113	0.044	0.130	0.076	B	292	...
31	11 36 12.35	-61 32 44.9	10.089	0.013	0.093	0.018	0.191	0.034	B	151	CD -60° 3626
32	11 35 05.96	-61 33 08.3	13.253	0.060	0.875	0.089	1.004	0.098	O
33	11 36 37.74	-61 33 10.9	10.991	0.016	0.055	0.022	0.156	0.039	B	177	...
34	11 36 04.39	-61 33 16.6	12.612	0.031	0.086	0.040	0.105	0.070	B
35	11 35 49.54	-61 33 18.3	12.719	0.033	0.109	0.042	0.146	0.072	B	135	...
36	11 36 22.69	-61 33 33.9	12.641	0.030	0.106	0.039	0.139	0.068	B	13	...
37	11 36 20.73	-61 33 41.3	12.563	0.030	0.110	0.038	0.153	0.066	B	12	...
38	11 36 11.25	-61 33 47.4	12.260	0.027	0.120	0.035	0.100	0.061	B	9	...
39	11 36 03.20	-61 33 54.3	13.096	0.039	0.710	0.057	0.898	0.068	O
40	11 36 51.74	-61 34 03.7	12.018	0.024	0.081	0.032	0.172	0.055	B	181	...
41	11 35 36.88	-61 34 04.9	10.619	0.015	0.050	0.021	0.151	0.037	B	130	CPD -60° 3088
42	11 36 38.40	-61 34 10.5	11.409	0.019	0.054	0.025	0.147	0.045	B	178	...
43	11 36 00.95	-61 34 17.4	11.733	0.021	0.108	0.028	0.143	0.049	B	140	...
44	11 36 44.23	-61 34 18.2	13.513	0.046	0.793	0.067	0.954	0.079	O	180	...
45	11 36 08.24	-61 34 19.3	10.685	0.015	0.049	0.021	0.140	0.037	B	8	...

TABLE 1—*Continued*

Star	RA (2000)	Dec (2000)	y	δy	$b - y$	$\delta(b - y)$	$y - H\alpha$	$\delta(y - H\alpha)$	Code	WEBDA	Identifier
46	11 36 40.44	-61 34 22.7	11.464	0.019	0.098	0.025	0.161	0.044	B	179	...
47	11 36 31.56	-61 34 25.6	8.528	0.009	0.076	0.014	0.470	0.028	Be	15	HD 306791
48	11 36 00.04	-61 34 27.0	12.172	0.026	0.084	0.034	0.146	0.058	B	139	...
49	11 35 54.42	-61 34 30.4	10.809	0.015	0.054	0.021	0.145	0.037	B	137	...
50	11 35 23.43	-61 34 44.7	12.225	0.028	0.763	0.042	0.936	0.049	O
51	11 36 31.86	-61 34 46.8	9.936	0.011	0.003	0.016	0.145	0.032	B	16	CPD -60°3158
52	11 36 04.92	-61 34 49.1	10.074	0.012	0.058	0.018	0.150	0.032	B	7	...
53	11 36 20.68	-61 34 59.4	12.359	0.027	0.133	0.035	0.179	0.059	B	19	...
54	11 35 35.86	-61 35 00.7	10.361	0.014	0.058	0.020	0.161	0.035	B	125	CPD -60°3083
55	11 36 15.87	-61 35 01.6	10.402	0.014	0.057	0.019	0.153	0.035	B
56	11 35 44.89	-61 35 05.0	12.595	0.031	0.101	0.040	0.167	0.068	B	127	...
57	11 36 12.03	-61 35 10.6	11.289	0.019	0.068	0.025	0.167	0.044	B	24	CPD -60°3134
58	11 35 14.99	-61 35 10.2	12.235	0.027	0.100	0.035	0.098	0.061	B	281	...
59	11 35 47.72	-61 35 11.1	11.955	0.025	0.817	0.039	0.988	0.045	O	129	...
60	11 36 29.57	-61 35 14.0	12.811	0.033	0.117	0.043	0.171	0.073	B	17	...
61	11 36 21.38	-61 35 15.0	9.581	0.012	0.072	0.018	0.218	0.031	Be?	20	...
62	11 35 46.47	-61 35 17.9	13.246	0.041	0.474	0.056	0.647	0.077	O	128	...
63	11 35 43.53	-61 35 18.6	13.644	0.048	0.519	0.066	0.955	0.082	O	126	...
64	11 36 25.51	-61 35 19.0	12.587	0.029	0.119	0.038	0.182	0.067	B	18	...
65	11 35 21.21	-61 35 20.4	11.777	0.022	0.099	0.029	0.166	0.051	B
66	11 36 20.77	-61 35 21.4	11.731	0.022	0.223	0.030	0.265	0.049	O	1076	...
67	11 36 08.97	-61 35 21.7	11.173	0.018	0.066	0.024	0.171	0.042	B	25	...
68	11 36 15.19	-61 35 22.4	12.083	0.025	0.081	0.033	0.103	0.058	B
69	11 36 04.55	-61 35 23.0	8.174	0.013	0.073	0.021	0.167	0.033	B
70	11 36 59.16	-61 35 31.4	12.889	0.050	0.609	0.071	0.935	0.084	O
71	11 36 26.36	-61 35 36.8	11.533	0.019	0.071	0.025	0.142	0.045	B
72	11 36 01.98	-61 35 38.1	12.638	0.031	0.110	0.040	0.162	0.068	B	4	...
73	11 36 09.56	-61 35 38.1	9.228	0.011	0.062	0.016	0.218	0.030	B	26	...
74	11 36 21.24	-61 35 38.4	10.661	0.015	0.057	0.021	0.162	0.037	B	1031	...
75	11 35 25.69	-61 35 38.7	12.467	0.029	0.109	0.038	0.139	0.065	B	121	...
76	11 36 22.05	-61 35 38.8	9.115	0.011	0.071	0.016	0.171	0.030	B	21	...
77	11 36 40.81	-61 35 41.1	11.357	0.019	0.096	0.025	0.177	0.043	B	195	...
78	11 36 18.29	-61 35 42.3	9.983	0.013	0.055	0.018	0.152	0.034	B	22	CPD -60°3137
79	11 35 32.66	-61 35 42.3	11.131	0.016	0.064	0.022	0.165	0.040	B	118	...
80	11 36 08.59	-61 35 42.5	12.720	0.033	0.162	0.043	0.212	0.071	O	1147	...
81	11 35 50.71	-61 35 46.8	12.772	0.033	0.120	0.043	0.161	0.073	B
82	11 36 10.08	-61 35 47.2	12.868	0.033	0.096	0.043	0.133	0.075	B	1164	...
83	11 36 11.86	-61 35 50.2	8.337	0.010	0.072	0.016	0.246	0.029	Be?	27	CPD -60°3128
84	11 36 03.57	-61 35 50.6	11.485	0.020	0.054	0.026	0.159	0.047	B	6	...
85	11 36 27.33	-61 35 52.7	12.774	0.033	0.100	0.042	0.089	0.074	B	40	...
86	11 36 10.44	-61 35 59.0	11.178	0.018	0.076	0.024	0.150	0.043	B	28	...
87	11 35 44.07	-61 36 04.4	11.635	0.021	0.082	0.028	0.169	0.049	B	114	...
88	11 35 48.87	-61 36 06.7	10.347	0.014	0.386	0.021	0.534	0.033	O
89	11 36 15.78	-61 36 08.1	11.086	0.017	0.073	0.023	0.144	0.042	B
90	11 36 26.84	-61 36 10.6	11.715	0.022	0.108	0.029	0.105	0.050	B

TABLE 1—*Continued*

Star	RA (2000)	Dec (2000)	y	δy	$b - y$	$\delta(b - y)$	$y - H\alpha$	$\delta(y - H\alpha)$	Code	WEBDA	Identifier
91	11 36 06.96	-61 36 12.6	12.872	0.033	0.105	0.043	0.156	0.073	B
92	11 35 55.45	-61 36 13.7	8.615	0.011	0.064	0.016	0.219	0.029	Be?	1	HD 100856
93	11 36 32.03	-61 36 17.2	12.683	0.033	0.481	0.045	0.529	0.064	O	44	...
94	11 36 49.34	-61 36 20.9	10.791	0.016	0.104	0.022	0.272	0.038	Be?	194	...
95	11 35 44.34	-61 36 23.3	12.144	0.024	0.098	0.032	0.152	0.056	B	113	...
96	11 36 32.10	-61 36 25.9	11.610	0.021	0.106	0.028	0.165	0.048	B	45	...
97	11 36 25.59	-61 36 26.1	11.892	0.022	0.102	0.029	0.141	0.052	B	42	...
98	11 36 21.85	-61 36 29.8	10.587	0.015	0.066	0.021	0.174	0.036	B	36	V848 Cen
99	11 36 09.07	-61 36 33.3	12.098	0.025	0.080	0.033	0.167	0.057	B	32	...
100	11 36 32.16	-61 36 38.0	12.765	0.033	0.042	0.042	0.114	0.075	B
101	11 36 10.86	-61 36 38.8	12.287	0.027	0.083	0.035	0.156	0.061	B	34	...
102	11 36 23.21	-61 36 40.4	11.566	0.019	0.089	0.025	0.174	0.045	B	38	...
103	11 35 35.38	-61 36 41.0	11.373	0.018	0.071	0.024	0.159	0.044	B	111	...
104	11 35 53.63	-61 36 42.6	12.785	0.033	0.155	0.043	0.166	0.073	O	109	...
105	11 36 09.43	-61 36 43.0	12.324	0.027	0.094	0.035	0.116	0.060	B	33	...
106	11 36 40.34	-61 36 45.4	12.861	0.037	1.073	0.059	1.248	0.059	O
107	11 36 19.02	-61 36 45.7	12.203	0.027	0.105	0.035	0.188	0.059	B
108	11 36 30.11	-61 36 47.6	12.269	0.027	0.104	0.035	0.126	0.061	B	43	...
109	11 36 59.44	-61 36 49.8	10.920	0.023	0.066	0.032	0.159	0.051	B	193	...
110	11 35 41.32	-61 36 56.2	10.520	0.013	0.048	0.018	0.140	0.035	B	107	CPD -60°3091
111	11 36 21.01	-61 36 58.3	10.236	0.013	0.078	0.018	0.166	0.034	B	52	...
112	11 36 18.85	-61 37 03.8	11.149	0.018	0.081	0.024	0.183	0.042	B
113	11 36 11.31	-61 37 07.2	12.763	0.033	0.111	0.043	0.177	0.073	B	61	...
114	11 36 16.30	-61 37 07.4	12.339	0.028	0.105	0.036	0.176	0.062	B
115	11 36 17.74	-61 37 08.6	11.554	0.021	0.106	0.028	0.165	0.048	B
116	11 36 18.75	-61 37 10.2	12.174	0.026	0.105	0.034	0.201	0.057	B
117	11 35 38.71	-61 37 13.7	13.235	0.041	0.666	0.059	0.881	0.072	O	105	...
118	11 36 33.08	-61 37 14.4	12.019	0.023	0.088	0.030	0.188	0.054	B
119	11 36 01.10	-61 37 18.4	10.099	0.012	0.065	0.018	0.164	0.033	B	81	...
120	11 36 25.96	-61 37 19.0	12.699	0.032	0.131	0.042	0.144	0.072	B	51	...
121	11 35 47.91	-61 37 19.6	12.242	0.027	0.086	0.034	0.173	0.058	B	108	...
122	11 36 10.74	-61 37 21.0	12.231	0.025	0.136	0.033	0.088	0.059	B	62	...
123	11 36 55.73	-61 37 21.6	11.732	0.022	0.317	0.030	0.472	0.046	O
124	11 36 02.65	-61 37 24.6	12.465	0.029	0.126	0.038	0.024	0.068	B	1200	...
125	11 36 14.40	-61 37 24.7	11.962	0.023	0.100	0.030	0.163	0.052	B	66	...
126	11 36 02.42	-61 37 26.4	12.470	0.029	0.068	0.038	0.218	0.064	Be?
127	11 36 21.94	-61 37 28.4	10.847	0.016	0.084	0.022	0.405	0.038	Be	53	...
128	11 35 35.73	-61 37 30.1	12.238	0.027	0.071	0.035	0.158	0.059	B	103	...
129	11 35 41.15	-61 37 32.5	12.329	0.027	0.103	0.035	0.179	0.059	B
130	11 36 14.05	-61 37 35.6	9.927	0.013	0.070	0.018	0.266	0.033	Be?	67	...
131	11 36 21.64	-61 37 38.0	11.376	0.019	0.090	0.025	0.171	0.045	B	54	...
132	11 36 46.91	-61 37 39.0	13.398	0.044	0.684	0.063	0.910	0.076	O	1238	...
133	11 36 10.16	-61 37 39.8	9.241	0.010	0.068	0.016	0.178	0.030	B	63	V846 Cen
134	11 36 47.27	-61 37 42.2	12.590	0.031	0.106	0.040	0.214	0.068	B
135	11 36 02.18	-61 37 43.6	12.872	0.035	0.128	0.045	0.150	0.076	B	84	...

TABLE 1—*Continued*

Star	RA (2000)	Dec (2000)	y	δy	$b - y$	$\delta(b - y)$	$y - H\alpha$	$\delta(y - H\alpha)$	Code	WEBDA	Identifier
136	11 36 08.41	-61 37 47.5	11.870	0.022	0.140	0.029	0.174	0.051	B	64	...
137	11 36 17.42	-61 37 48.4	12.120	0.024	0.138	0.032	0.205	0.055	B
138	11 36 05.84	-61 37 51.4	11.442	0.018	0.088	0.024	0.172	0.044	B
139	11 36 41.89	-61 37 53.7	11.050	0.017	0.084	0.023	0.227	0.040	Be?	204	...
140	11 36 23.89	-61 38 02.9	12.848	0.033	0.157	0.043	0.141	0.074	O	69	...
141	11 35 45.12	-61 38 03.4	12.822	0.033	0.145	0.043	0.156	0.074	B	99	...
142	11 35 08.53	-61 38 06.9	11.762	0.031	0.076	0.041	0.167	0.066	B
143	11 35 52.25	-61 38 07.5	9.634	0.012	0.056	0.018	0.168	0.031	B	97	CPD -60°3098
144	11 36 51.60	-61 38 08.2	11.284	0.026	1.199	0.044	1.300	0.040	O	202	...
145	11 36 38.82	-61 38 11.7	12.215	0.027	0.125	0.035	0.161	0.059	B	205	...
146	11 36 08.73	-61 38 12.8	10.669	0.014	0.152	0.021	0.179	0.036	O
147	11 35 52.37	-61 38 15.2	11.839	0.023	0.094	0.030	0.193	0.051	B	1086	...
148	11 35 57.02	-61 38 15.6	11.213	0.018	0.078	0.025	0.189	0.043	B	87	...
149	11 36 59.58	-61 38 22.3	12.021	0.033	0.127	0.043	0.144	0.074	B	208	...
150	11 35 31.33	-61 38 24.5	12.485	0.028	0.119	0.037	0.155	0.063	B
151	11 35 46.89	-61 38 25.3	12.060	0.025	0.081	0.033	0.162	0.056	B	98	...
152	11 36 11.07	-61 38 28.5	11.243	0.017	0.083	0.023	0.145	0.042	B
153	11 36 13.20	-61 38 36.4	12.918	0.036	0.672	0.052	0.854	0.064	O	77	...
154	11 36 08.02	-61 38 38.2	9.985	0.013	0.071	0.018	0.663	0.032	Be	88	V845 Cen
155	11 36 46.00	-61 38 37.7	12.362	0.028	0.117	0.036	0.182	0.062	B
156	11 36 36.98	-61 38 42.8	12.792	0.033	0.175	0.043	0.143	0.073	O	206	...
157	11 36 05.44	-61 38 48.8	12.850	0.034	0.133	0.044	0.183	0.075	B	89	...
158	11 36 04.27	-61 38 53.8	11.886	0.023	0.085	0.030	0.165	0.052	B	90	...
159	11 35 59.53	-61 38 58.6	11.776	0.021	0.096	0.028	0.155	0.049	B	93	...
160	11 36 48.96	-61 38 58.5	12.980	0.051	0.133	0.065	0.144	0.107	B
161	11 36 21.10	-61 39 03.3	9.084	0.011	0.056	0.016	0.167	0.030	B	70	CD -60°3629
162	11 36 34.47	-61 39 13.2	12.581	0.031	0.119	0.040	0.120	0.069	B
163	11 36 33.56	-61 39 14.1	13.528	0.047	0.773	0.068	0.997	0.079	O
164	11 36 03.41	-61 39 15.3	11.844	0.023	0.087	0.030	0.157	0.052	B	91	...
165	11 36 00.22	-61 39 16.8	12.302	0.026	0.115	0.034	0.129	0.059	B
166	11 36 37.72	-61 39 23.4	12.470	0.029	0.107	0.038	0.137	0.064	B	214	...
167	11 35 16.16	-61 39 27.1	12.046	0.024	0.422	0.034	0.590	0.049	O	270	...
168	11 36 28.07	-61 39 30.8	12.829	0.033	0.116	0.043	0.150	0.074	B	71	...
169	11 35 39.12	-61 39 37.0	12.012	0.024	0.159	0.032	0.172	0.055	O	100	...
170	11 35 52.00	-61 39 39.6	10.676	0.015	0.047	0.021	0.150	0.037	B	94	HD 306795
171	11 36 54.96	-61 39 39.2	11.567	0.019	0.081	0.025	0.169	0.046	B	211	...
172	11 36 11.09	-61 39 42.0	12.158	0.025	0.140	0.033	0.088	0.058	B
173	11 36 29.91	-61 39 47.1	12.406	0.029	0.124	0.038	0.214	0.063	B	233	...
174	11 36 34.27	-61 39 49.8	12.600	0.031	0.128	0.040	0.169	0.068	B	217	...
175	11 36 36.02	-61 39 57.9	11.848	0.023	0.093	0.030	0.178	0.052	B	218	...
176	11 36 50.47	-61 40 00.8	9.133	0.011	0.053	0.016	0.144	0.030	B	212	HD 100989
177	11 36 50.33	-61 40 07.6	11.924	0.024	0.377	0.033	0.506	0.049	O	1088	...
178	11 36 48.63	-61 40 10.0	11.883	0.023	0.080	0.030	0.143	0.053	B	213	...
179	11 36 24.40	-61 40 23.9	10.468	0.014	0.055	0.020	0.161	0.035	B	234	...
180	11 36 16.50	-61 40 34.6	13.377	0.043	0.397	0.058	0.674	0.080	O	74	...

TABLE 1—*Continued*

Star	RA (2000)	Dec (2000)	y	δy	$b - y$	$\delta(b - y)$	$y - H\alpha$	$\delta(y - H\alpha)$	Code	WEBDA	Identifier
181	11 36 02.94	-61 40 36.7	13.215	0.040	0.530	0.056	0.741	0.074	O
182	11 35 42.12	-61 40 39.2	11.424	0.025	0.999	0.040	1.182	0.041	O	258	...
183	11 36 05.73	-61 40 40.9	10.302	0.015	0.364	0.022	0.519	0.034	O	95	...
184	11 36 18.18	-61 40 42.0	10.837	0.015	0.080	0.021	0.147	0.037	B
185	11 35 42.89	-61 40 53.4	10.965	0.017	0.068	0.023	0.160	0.041	B	257	HD 306796
186	11 36 41.44	-61 40 58.0	12.836	0.034	0.107	0.044	0.120	0.076	B	221	...
187	11 35 40.30	-61 41 02.6	13.276	0.043	0.901	0.064	1.116	0.069	O	259	...
188	11 36 37.73	-61 41 02.5	12.556	0.031	0.230	0.040	0.109	0.068	O	220	...
189	11 36 37.58	-61 41 04.1	12.544	0.030	0.294	0.040	0.053	0.069	O	1170	...
190	11 35 37.15	-61 41 09.7	11.784	0.021	0.088	0.028	0.185	0.049	B	260	...
191	11 36 18.32	-61 41 12.9	13.323	0.043	1.169	0.071	1.324	0.067	O
192	11 36 12.13	-61 41 18.7	11.526	0.019	0.120	0.025	0.146	0.046	B
193	11 35 47.47	-61 41 24.5	12.998	0.038	0.857	0.057	1.064	0.062	O	1172	...
194	11 36 29.59	-61 41 35.2	12.926	0.050	0.107	0.065	0.163	0.104	B	231	...
195	11 36 21.10	-61 41 40.6	12.684	0.031	0.164	0.041	0.219	0.068	O
196	11 36 09.37	-61 41 41.5	9.444	0.011	0.059	0.016	0.163	0.031	B	239	HD 306798
197	11 35 50.86	-61 41 56.4	12.120	0.025	0.093	0.033	0.153	0.057	B	253	...
198	11 35 15.15	-61 41 59.5	10.428	0.014	0.117	0.020	0.911	0.032	Be	264	HD 306657
199	11 35 56.96	-61 42 04.8	13.821	0.075	0.921	0.113	0.983	0.120	O	250	...
200	11 36 05.48	-61 42 06.0	9.700	0.011	0.065	0.016	0.369	0.030	B	240	HD 306797
201	11 36 42.24	-61 42 13.4	11.160	0.021	0.755	0.033	0.933	0.038	O
202	11 36 58.38	-61 42 18.8	13.493	0.066	1.072	0.104	1.679	0.091	O	1390	...
203	11 36 58.39	-61 42 18.9	13.498	0.067	1.132	0.106	1.684	0.092	O	225	...
204	11 35 15.97	-61 42 20.9	12.240	0.028	0.779	0.043	0.960	0.050	O	263	...
205	11 35 57.08	-61 42 22.1	13.599	0.068	0.822	0.100	0.968	0.110	O	249	...
206	11 36 41.64	-61 42 22.2	10.800	0.015	0.151	0.021	0.227	0.036	O	229	...
207	11 36 37.71	-61 42 26.5	12.016	0.027	0.915	0.043	1.102	0.046	O
208	11 36 47.25	-61 42 31.5	13.433	0.064	0.833	0.094	0.973	0.106	O
209	11 35 43.54	-61 42 47.2	13.560	0.047	0.716	0.067	0.977	0.080	O

NOTE.—For each star observed in NGC 3766, we give the right ascension (RA) and declination (Dec) for the epoch 2000. We also provide the y magnitude, the $b - y$ and $y - H\alpha$ colors, and the error for each. The code is used to label definite Be stars (Be), possible Be stars (Be?), B-type stars (B), and other stars in the field (O). Finally, the WEBDA number and other identifiers are provided where available.